NONLINEAR OBSERVERS FOR GYRO CALIBRATION

Julie Thienel* and Robert M. Sanner†

Nonlinear observers for gyro calibration are presented. The first observer estimates a constant gyro bias. The second observer estimates scale factor errors. The third observer estimates the gyro alignment for three orthogonal gyros. The convergence properties of all three observers are discussed. Additionally, all three observers are coupled with a nonlinear control algorithm. The stability of each of the resulting closed loop systems is analyzed. Simulated test results are presented for each system.

INTRODUCTION

Gyroscopes, also known as Inertial Reference Units (IRU) or gyros, are part of the attitude control system of most three-axis stabilized spacecraft. They measure the spacecraft angular rate. Unfortunately, the gyro measurements are corrupted by errors in alignment, scale factor, and bias, as well as random noise.[1] Several algorithms for estimating the errors, as well as the noise charac- teristics, are available.[2–8] Most algorithms rely on linear techniques, and are not coupled directly with the spacecraft control.

The published nonlinear methods tend to follow a similar Lyapunov development to determine stability, most are driven by a measurable attitude error. Alonso, et al. in Ref. 9 develop a nonlinear observer for relative attitude and rate estimation with an application to spacecraft formation flying. Salcudean in Ref. 10 develops a nonlinear observer for angular rate estimation. Both observers are driven by a computed attitude error. However, in order to estimate the rate, both observers require knowledge or estimation of spacecraft torques. The stability of the observer developed by Salcudean requires an assumption that the system eventually behaves as a linear time invariant system. In Ref. 11, Vik, et al. develop an angular velocity observer, in addition to a position and velocity observer, for use in a Global Positioning System (GPS)/Inertial Navigation System (INS). The angular velocity observer is actually a nonlinear observer for gyro calibration. The observer is designed to estimate corrections to the gyro measurements, particularly misalignment and scale factor corrections, along with gyro biases. The misalignment and scale factor errors are assumed to be small. All the error terms are modelled as exponentially decaying, first-order equations. The Lyapunov analysis proves that the observer, given the above assumptions, is exponentially stable. A closed-loop analysis of the observer, coupled with a controller, is not presented. Nonlinear observers for gyro bias estimation are presented by Boskovic, et al. in Refs. 12 and 13. In Ref. 12, the bias is assumed to be constant, which differs from the exponentially decaying model of Ref. 11. However, the bias is assumed to lie in a small, bounded set. Second order terms are neglected in the observer development and in the Lyapunov proof of stability. The observer is coupled with a controller, designed to drive the spacecraft rates to zero, and the spacecraft body coordinates to the inertial coordinates. With the second order terms neglected, the closed loop system is stable for the single scenario presented. In Ref. 13, the gyro bias observer is designed for use in attitude

*NASA Goddard Space Flight Center, Flight Dynamics Analysis Branch, Greenbelt, MD 20771, phone: 301-286-9033, fax: 301-286-0369, email: julie.thienel@nasa.gov

†University of Maryland, Department of Aerospace Engineering, College Park, Maryland, 20742 phone: 301-405-1928, fax: 301-314-9001, email: rmsanner@eng.umd.edu

tracking. Here the bias observer is driven by a computed attitude error, as in Refs. 9, 10, and 11. However, the attitude error is computed as a vector difference, rather than a rotational error, without consideration to the normality constraint of the attitude. An adaptive tracking controller is coupled to the observer. The convergence proof for this observer assumes that the vehicle attitude never passes through ±180 degrees, and the stability of the coupled observer/controller/spacecraft dynamics is not formally established.

As the above discussion indicates, combined observer-controller designs for the attitude control of rigid flight vehicles are a subject of active research.[11-13] Successful design of such architectures is complicated by the fact that there is, in general, no separation principle for nonlinear systems. In contrast to linear systems, 'certainty equivalence' substitution of the states from an exponentially converging observer into a nominally stabilizing, state feedback control law does not necessarily guarantee stable closed-loop operation for the coupled systems.[14, 15] In this work, one version of this problem is considered, in particular, the task of forcing the attitude of a rigid vehicle to asymptotically track a (time-varying) reference attitude using feedback from rate sensors with persistent nonzero errors.

The next section introduces the terminology used throughout the document, as well as an overview of a nonlinear attitude control law. Next, the development of nonlinear observers for the case of constant gyro bias, constant scale factor error, and constant alignment error are presented. Each observer is combined with the nonlinear control scheme for attitude control of a spacecraft. Simulation results are presented for each of the observers and for each of the closed loop systems. The paper concludes with a summary and discussion of future work.

TERMINOLOGY

The attitude of a spacecraft can be represented by a quaternion, consisting of a rotation angle and unit rotation vector e, known as the Euler axis, and a rotation ϕ about this axis so that[16]

$$q = \left[\begin{array}{c} e \sin(\frac{\phi}{2}) \\ \cos(\frac{\phi}{2}) \end{array} \right] = \left[\begin{array}{c} \varepsilon \\ \eta \end{array} \right] \tag{1}$$

where q is the quaternion, partitioned into a vector part, ε, and a scalar part, η. Typically, in spacecraft attitude applications, the quaternion represents the rotation from an inertial coordinate system to the spacecraft body coordinate system. Note that $||\mathbf{q}|| = 1$ by definition. The rotation matrix for a specific attitude can be computed from the quaternion components as[16]

$$R(q) = (\eta^2 - \varepsilon^T \varepsilon)I + 2\varepsilon\varepsilon^T - 2\eta S(\varepsilon) \tag{2}$$

where I is a 3x3 identity matrix and $S(\varepsilon)$ is a matrix representation of the vector cross product operation.

$$S(\varepsilon) = \left[\begin{array}{ccc} 0 & -\varepsilon_z & \varepsilon_y \\ \varepsilon_z & 0 & -\varepsilon_x \\ -\varepsilon_y & \varepsilon_x & 0 \end{array} \right]$$

The rotation matrix is orthogonal, $R^T R = I$. Note also that $R(q)\varepsilon = \varepsilon$.

The relative orientation between two coordinate frames is computed as[17]

$$\bar{q} = \left[\begin{array}{c} \bar{\varepsilon} \\ \bar{\eta} \end{array} \right] = q_1 \otimes q_2^{-1} = \left[\begin{array}{cc} \eta_2 I - S(\varepsilon_2) & -\varepsilon_2 \\ \varepsilon_2^T & \eta_2 \end{array} \right] \left[\begin{array}{c} \varepsilon_1 \\ \eta_1 \end{array} \right] \tag{3}$$

Where $\bar{q}$ defines the rotation from the frame defined by q_2 to the frame defined by q_1. Note that $||\bar{\varepsilon}|| = 0$, $\bar{\eta} = \pm 1$ indicates that the frame 2 is aligned with frame 1.

2

The kinematic equation for the quaternion is given as

$$\dot{q}(t) = \begin{bmatrix} \dot{\varepsilon}(t) \\ \dot{\eta}(t) \end{bmatrix} = \frac{1}{2}Q(q(t))\omega(t)$$ (4)

where $\omega(t)$ is the spacecraft angular velocity in body coordinates and

$$Q(q(t)) = \begin{bmatrix} \eta(t)\mathbf{I} + S(\varepsilon(t)) \\ -\varepsilon(t) \end{bmatrix} = \begin{bmatrix} Q_1(q(t)) \\ -\varepsilon(t)^T \end{bmatrix}$$ (5)

where, by inspection, $Q_1(q(t)) = \eta(t)\mathbf{I} + S(\varepsilon(t))$. The angular velocity, $\omega(t)$, is typically measured by a gyro, which can be corrupted from various sources, such as errors in bias, misalignment, and scale factor, and noise. The measured angular velocity can be written as[1]

$$\omega_g(t) = \Gamma R^T(q_g)\omega(t) + b_g(t) + \nu_{\omega g}(t)$$ (6)

where $\omega_g(t)$ is the angular velocity in the gyro coordinate frame, Γ is a diagonal matrix of scale factors, or more traditionally, a matrix containing scale factor errors (i.e. the main diagonal contains components $1 + \gamma_i$, where γ_i is the scale factor error for gyro i). This work considers only the case of three, orthogonal gyros. Therefore, $R(q_g)$ is an orthogonal gyro alignment matrix, a transformation from a gyro coordinate frame to the spacecraft body frame (note that for a non-orthogonal gyro triad, this matrix cannot be represented with a quaternion). The (possibly time varying) gyro bias is given by $b_g(t)$, in the gyro coordinate frame, and finally, $\nu_{\omega g}(t)$ is a zero mean noise vector, also in the gyro coordinate frame.

Solving (6) for $\omega(t)$,

$$\omega(t) = C(\omega_g(t) - b_g(t) - \nu_{\omega g}(t))$$ (7)

where $C = (\Gamma R(q_g)^T)^{-1} = R(q_g)\Gamma^{-1}$ for three orthogonal gyros. Rewriting (7) as

$$\omega(t) = C\omega_g(t) - b(t) - \nu(t)$$ (8)

where $b(t) = C\omega_g(t)$ is the effective gyro bias in the spacecraft body frame, and, similarly, $\nu(t)$ is the effective noise in the spacecraft body frame. If Γ, q_g, and $b(t)$ are known, an unbiased estimate of $\omega(t)$ is

$$\hat{\omega}(t) = C\omega_g(t) - b(t)$$

This paper considers the case where Γ, q_g, and $b(t)$ are *unknown* and of *arbitrary* size.

In this work, the gyro alignment and scale factors are assumed to be constant. In other words,

$$\dot{q}_g(t) = \mathbf{0}$$ (9)

$$\dot{\gamma}_i(t) = 0$$ (10)

The bias is assumed to be constant.

$$\dot{b}(t) = \mathbf{0}$$ (11)

The effects of uniformly bounded noise on the bias and angular velocity are considered in Ref. 20.

If $\hat{b}(t)$, $\hat{q}_g(t)$, and $\hat{\Gamma}_I(t)$ are estimates of the unknown bias, alignment quaternion, and inverted scale factor matrix, respectively, an estimate of the angular velocity is given as

$$\hat{\omega}(t) = R(\hat{q}_g(t))\hat{\Gamma}_I(t)\omega_g(t) - \hat{b}(t)$$ (12)

For the case of bias error only (assuming the alignment and scale factor matrices are known), (12) becomes

$$\hat{\omega}(t) = R(q_g)\Gamma^{-1}\omega_g(t) - \hat{b}(t)$$ (13)

3

The equation is rewritten accordingly for a pure alignment estimate (with known scale factor and zero bias), as

$$\hat{\omega}(t) = R(\hat{q}_g(t))\Gamma^{-1}\omega_g(t) \tag{14}$$

where $R(\hat{q}_g(t))$ represents the rotation from gyro coordinates to an estimated body frame. Finally, for an estimate of the inverted scale factor matrix (12) (with a known alignment and zero bias) becomes

$$\hat{\omega}(t) = R(q_g)\hat{\Gamma}_I(t)\omega_g(t) \tag{15}$$

or similarly for any other combination of terms.

The error terms for each of the calibration parameters are defined as

$$\tilde{b}(t) = b - \hat{b}(t) \tag{16}$$

$$\tilde{q}_g(t) = q_g \otimes \hat{q}_g(t)^{-1} \tag{17}$$

$$\tilde{\gamma}_I(t) = \gamma_I - \hat{\gamma}_I(t) \tag{18}$$

where $\tilde{\gamma}_I(t)$ is a scale factor error vector defined as the difference between the inverted true scale factors and the estimates. This work examines each error source separately.

Nonlinear Control Algorithm

The attitude dynamics for a rigid spacecraft are given as

$$H\dot{\omega}(t) - S(H\omega(t))\omega(t) = u(t) \tag{19}$$

H is a constant, symmetric inertia matrix and $u(t)$ is the applied external torque, for example, from attached rocket thrusters. The goal of the control law is to force the actual, measured attitude $q(t)$ to asymptotically track a (generally) time-varying desired attitude $q_d(t)$ and angular velocity $\omega_d(t)$, related for consistency by (4) as

$$\dot{q}_d(t) = \frac{1}{2}Q(q_d(t))\omega_d(t) \tag{20}$$

It is assumed that $\omega_d(t)$ is bounded and differentiable with $\dot{\omega}_d(t)$ also bounded.

The commanded attitude tracking error is computed with (3) as

$$\tilde{q}_c(t) = \left[\begin{array}{c} \tilde{\varepsilon}_c(t) \\ \tilde{\eta}_c(t) \end{array} \right] = q(t) \otimes q_d^{-1}(t) \tag{21}$$

Correspondingly, the rate tracking error is

$$\tilde{\omega}_c(t) = \omega(t) - R(\tilde{q}_c(t))\omega_d(t) \tag{22}$$

With these definitions, the tracking error obeys the kinematic differential equation[17]

$$\dot{\tilde{q}}_c(t) = \frac{1}{2}Q(\tilde{q}_c(t))\tilde{\omega}_c(t) \tag{23}$$

A nonlinear tracking control strategy proposed by Egeland and Godhavn in Ref. 19 utilizes the control law

$$u(t) = -K_D s(t) + H\alpha_r(t) - S(H\omega(t))\omega_r(t) \tag{24}$$

K_D is any symmetric, positive definite matrix and $s(t)$ is an error defined as

$$s(t) = \tilde{\omega}_c(t)t + \lambda\tilde{\varepsilon}_c(t) = \omega(t) - \omega_r(t) \tag{25}$$

4

where λ is any positive constant. The reference angular velocity $\omega_r(t)$ is computed as

$$\omega_r(t) = R(\tilde{q}_c(t))\omega_d(t) - \lambda\tilde{\varepsilon}_c(t) \tag{26}$$

and

$$\alpha_r(t) = \dot{\omega}_r(t) = R(\tilde{q}_c(t))\dot{\omega}_d(t) - S(\tilde{\omega}_c(t))R(\tilde{q}_c(t))\omega_d(t) - \lambda Q_1(\tilde{q}_c(t))\tilde{\omega}_c(t)t \tag{27}$$

Asymptotically perfect tracking, i.e. $\tilde{\varepsilon}_c(t) \to 0$, $\tilde{\omega}_c(t) \to 0$, is obtained with the above control scheme, given noise free measurements of the states $\omega(t)$ and $q(t)$. In this work we investigate the application of this control algorithm, given the uncertainties in the angular velocity as quantified above.

NONLINEAR OBSERVERS

Following the observer proposed in Ref. 11, a state observer for the attitude in the case of either gyro bias or scale factor error is proposed as

$$\dot{\hat{q}}(t) = \frac{1}{2}Q(\hat{q}(t))R(\tilde{q}_o(t))^T[\hat{\omega}(t) + k\tilde{\varepsilon}_o(t)\text{sign}(\tilde{\eta}_o(t))] \tag{28}$$

where $\hat{\omega}(t)$ is given in (13) for the case of gyro bias and in (15) for the case of scale factor error.

The proposed observers for the gyro bias and scale factor errors are
Gyro bias:

$$\dot{\hat{b}} = -\frac{1}{2}\tilde{\varepsilon}_o(t)\text{sign}(\tilde{\eta}_o(t)) \tag{29}$$

Scale factor:

$$\dot{\hat{\gamma}}_{Ii}(t) = \frac{1}{2}\omega_{gi}(t)\tilde{\varepsilon}_{oi}(t)\text{sign}(\tilde{\eta}_o(t)) \tag{30}$$

In the case of alignment error, the proposed attitude observer contains an additional term. The attitude and alignment observers are given as

$$\dot{\hat{q}}(t) = \frac{1}{2}Q(\hat{q}(t))R(\tilde{q}_o(t))^T[\hat{\omega}(t) + k(t)\tilde{\varepsilon}_o(t)sign(\tilde{\eta}_o(t)) + k_1(t)\text{sign}(\tilde{\varepsilon}_o(t))\text{sign}(\tilde{\eta}_o(t))] \tag{31}$$

$$\dot{\hat{q}}_g(t) = \frac{1}{2}Q(\hat{q}_g(t))R(\hat{q}_g(t))^T[(I - R(\tilde{q}_o(t)))R(\hat{q}_g(t))\omega_g(t)] \tag{32}$$

where $\hat{\omega}(t)$ is as given in (14). The scalar gains $k > 0$, $k(t) > 0$, and $k_1(t) > 0$ are defined below.

For the gyro bias observer, the alignment and scale factor are assumed to be known. The same is true for the scale factor and alignment observers (the other components are assumed to be known).

Essentially, $\hat{q}(t)$ is a prediction of the attitude at time t, propagated with the kinematic equation using the measured angular velocity and the current estimate of the error source, either gyro bias, scale factor, or alignment estimate. The attitude error is the relative orientation between the predicted attitude provided by (28) or (31) and the true attitude provided by the measured attitude, $q(t)$. The attitude error is computed using (3) as

$$\tilde{q}_o(t) = \left[\begin{array}{c} \tilde{\varepsilon}_o(t) \\ \tilde{\eta}_o(t) \end{array} \right] = q(t) \otimes \hat{q}(t_0)^{-1} \tag{33}$$

In (28) and (31) the term $R(\tilde{q}_o(t))^T$ transforms the angular velocity terms from the body frame to the observer frame.

In the scale factor observer (30), $\tilde{\varepsilon}_{oi}(t)$ are the three elements of $\tilde{\varepsilon}_o(t)$. The estimated scale factor components, $\hat{\gamma}_{Ii}(t)$ with $i = x, y, z$, are estimates of the inverse of the true scale factor components. Only scale factor estimates corresponding to non-zero $\omega_{gi}(t)$ are included in (30). The components $\hat{\gamma}_{Ii}(t)$ form the main diagonal of the matrix $\hat{\Gamma}_I(t)$ in (15). Note that the estimated scale factors, $\hat{\gamma}_{Ii}(t)$, are never inverted in the observer (or in the controller to follow), so dividing by zero is not a possibility.

In the alignment observer (32), the quaternion, $\hat{q}_g(t)$, is the estimated gyro alignment quaternion, transforming from gyro coordinates to an estimated body frame. The alignment error is given in (17). The term $R(\hat{q}_g(t))^T$ transforms the angular velocity term from the gyro frame to an estimated body frame.

In the case of pure bias error, the kinematic equation for $\tilde{q}_o(t)$ is given as

$$\dot{\tilde{q}}_o(t) = \frac{1}{2} \begin{bmatrix} Q_1(\tilde{q}_o(t)) \\ -\tilde{\varepsilon}_o(t)^T \end{bmatrix} (-\bar{b}(t) - k\tilde{\varepsilon}_o(t)\text{sign}(\tilde{\eta}_o(t))) \tag{34}$$

where $\bar{b}(t)$ obeys the differential equation

$$\dot{\bar{b}}(t) = \frac{1}{2}\tilde{\varepsilon}_o(t)\text{sign}(\tilde{\eta}_o(t)) \tag{35}$$

Note that the equilibrium states for (34) and (35) are

$$\begin{bmatrix} \tilde{q}_o(t)^T & \bar{b}(t)^T \end{bmatrix} = \begin{bmatrix} 0 & 0 & 0 & \pm 1 & 0 & 0 & 0 \end{bmatrix}$$

Ref. 20 proves that for any measured angular velocity, $\omega_g(t)$, the equilibrium states of the system (34) and (35) are exponentially stable. In particular, $\hat{b}(t) \to b$ exponentially fast from any initial conditions $\hat{q}(t_0)$ and $\hat{b}(t_0)$. Additionally, Ref. 20 considers the effect of bounded noise on both the bias and angular velocity. Again, the observers are found to be exponentially stable to within a ball determined by the standard deviations of the noise terms.

For pure scale factor errors, the derivatives of the attitude error, $\tilde{q}_o(t)$, and the scale factor error components are

$$\dot{\tilde{q}}_o(t) = \frac{1}{2} \begin{bmatrix} Q_1(\tilde{q}_o(t)) \\ -\tilde{\varepsilon}_o(t)^T \end{bmatrix} (\Gamma^{-1}\omega_g(t) - \hat{\Gamma}_I(t)\omega_g(t) - k\tilde{\varepsilon}_o(t)\text{sign}(\tilde{\eta}_o(t))) \tag{36}$$

$$\dot{\tilde{\gamma}}_{Ii}(t) = -\frac{1}{2}\omega_{gi}(t)\tilde{\varepsilon}_{oi}(t)\text{sign}(\tilde{\eta}_o(t)) \qquad \cdot \tag{37}$$

where again, $i = x, y, z$. Γ^{-1} is a diagonal matrix, containing the inverse of each of the true scale factors, defined as γ_{Ii}, on the main diagonal. The scale factor errors are defined as $\tilde{\gamma}_{Ii}(t) = \gamma_{Ii} - \hat{\gamma}_{Ii}(t)$, with $\tilde{\Gamma}_I(t)$ given as

$$\tilde{\Gamma}_I(t) = \begin{bmatrix} \tilde{\gamma}_{Ix}(t) & 0 & 0 \\ 0 & \tilde{\gamma}_{Iy}(t) & 0 \\ 0 & 0 & \tilde{\gamma}_{Iz}(t) \end{bmatrix}$$

The difference in angular velocity terms in (36) is then

$$\Gamma^{-1}\omega_g(t) - \hat{\Gamma}_I(t)\omega_g(t) = \tilde{\Gamma}_I(t)\omega_g(t) = \Omega_g(t)\tilde{\gamma}_I(t)$$

where $\Omega_g(t)$ is a diagonal matrix with the components of $\omega_g(t)$ on the main diagonal and $\tilde{\gamma}_I(t)$ is a vector containing the components $\tilde{\gamma}_{Ii}(t)$. (36) can then be rewritten as

$$\dot{\tilde{q}}_o(t) = \frac{1}{2} \begin{bmatrix} Q_1(\tilde{q}_o(t)) \\ -\tilde{\varepsilon}_o(t)^T \end{bmatrix} (\Omega_g(t)\tilde{\gamma}_I(t) - k\tilde{\varepsilon}_o(t)sign(\tilde{\eta}_o(t))) \tag{38}$$

6

Note that the equilibrium states for (37) and (38) are

$$\begin{bmatrix} \tilde{q}_o(t)^T & \tilde{\gamma}_I(t)^T \end{bmatrix} = \begin{bmatrix} 0 & 0 & 0 & \pm 1 & 0 & 0 & 0 \end{bmatrix}$$

In the case of alignment error, the kinematic equation for the attitude error quaternion is

$$\dot{\tilde{q}}_o(t) = \frac{1}{2} \begin{bmatrix} Q_1(\tilde{q}_o(t)) \\ -\tilde{\varepsilon}_o(t)^T \end{bmatrix} (R(q_g)\omega_g(t) - R(\hat{q}_g(t))\omega_g(t) - k(t)\tilde{\varepsilon}_o(t)\text{sign}(\tilde{\eta}_o(t))$$
$$- k_1(t)\text{sign}(\tilde{\varepsilon}_o(t))\text{sign}(\tilde{\eta}_o(t))) \tag{39}$$

Since the true alignment is constant, the angular velocity associated with the kinematic equation for the true alignment quaternion is zero. The kinematic equation for the alignment error quaternion is therefore

$$\dot{\tilde{q}}_g(t) = \frac{1}{2} \begin{bmatrix} Q_1(\tilde{q}_g(t)) \\ -\tilde{\varepsilon}_g(t)^T \end{bmatrix} [(R(\tilde{q}_o(t)) - I)R(\hat{q}_g(t))\omega_g(t)] \tag{40}$$

Since $R(q_g) = R(\tilde{q}_g(t))R(\hat{q}_g(t))$, where $R(\tilde{q}_g(t))$ represents the rotation from the estimated body frame to the actual body frame, (39) becomes

$$\dot{\tilde{q}}_o(t) = \frac{1}{2} \begin{bmatrix} Q_1(\tilde{q}_o(t)) \\ -\tilde{\varepsilon}_o(t)^T \end{bmatrix} [(R(\tilde{q}_g(t)) - I)R(\hat{q}_g(t))\omega_g(t) - k(t)\tilde{\varepsilon}_o(t)\text{sign}(\tilde{\eta}_o(t))$$
$$- k_1(t)\text{sign}(\tilde{\varepsilon}_o(t))\text{sign}(\tilde{\eta}_o(t))] \tag{41}$$

Note that the equilibrium state for each of the error quaternions, $\tilde{q}_o(t)$ in (41) and $\tilde{q}_g(t)$ in (40), is the identity quaternion, $[0\ 0\ 0\ \pm 1]$.

Stability of Scale Factor Observer

The proof follows that of the gyro bias observer.[20] Chose a Lyapunov function as

$$V_o(t) = \frac{1}{2} \sum_{i=1}^{3} \tilde{\gamma}_{Ii}(t)^2 + \frac{1}{2} \begin{cases} (\tilde{\eta}_o(t) - 1)^2 + \tilde{\varepsilon}_o(t)^T\tilde{\varepsilon}_o(t) & \tilde{\eta}_o(t) \geq 0 \\ (\tilde{\eta}_o(t) + 1)^2 + \tilde{\varepsilon}_o(t)^T\tilde{\varepsilon}_o(t) & \tilde{\eta}_o(t) < 0 \end{cases} \tag{42}$$

$V_o(t)$ is continuous. Noting that $\tilde{\varepsilon}_o(t)^T\dot{\tilde{\varepsilon}}_o(t) + \tilde{\eta}_o(t)\dot{\tilde{\eta}}_o(t) = 0$, as with the gyro bias analysis, the derivative of $V_o(t)$ (including the left and right derivatives of $\tilde{\eta}_o(t) = 0$) yields, for all $t \geq t_0$

$$\dot{V}_o(t) = -\frac{k}{2}\tilde{\varepsilon}_o(t)^T\tilde{\varepsilon}_o(t)$$

This establishes that $\tilde{\varepsilon}_o(t)$, $\tilde{\eta}_o(t)$, and $\tilde{\gamma}_{Ii}(t)$, are globally, uniformly bounded. $V_o(t)$ is a continuous, twice differentiable function with $\ddot{V}_o(t)$ bounded, given that $\omega_g(t)$ is bounded. Barbalat's lemma[15] then shows that $\|\tilde{\varepsilon}_o(t)\| \to 0$ as $t \to \infty$.

If $\omega_g(t)$ is bounded, all the signals in (37) and (38) are bounded. The system is, as in the gyro bias case, analyzed as a linear time varying system, $\dot{x}(t) = A(t)x(t)$.[14] If all the components of $\omega_g(t)$ are nonzero, $A(t)$ is given as

$$A(t) = \begin{bmatrix} -\frac{k}{2}\text{sign}(\tilde{\eta}_o(t))Q_1(\tilde{q}_o(t)) & \frac{1}{2}Q_1(\tilde{q}_o(t))\Omega_g(t) \\ -\frac{1}{2}\text{sign}(\tilde{\eta}_o(t))\Omega_g(t) & 0 \end{bmatrix}$$

If any of the components of $\omega_g(t)$ are zero, the system is reduced in dimension according to the non-zero components of $\omega_g(t)$.

The development proceeds like that for the gyro bias in Ref. 20, under the assumption that $\omega_g(t)$ is at least bounded. The equilibrium point $x(t) = 0$ of the equivalent system is exponentially

stable if the pair $(A(t), C)$ is uniformly completely observable (UCO). Rewriting $\dot{V}_o(t)$ as $\dot{V}_o(t) = -x(t)^T C^T C x(t) \leq 0$, C is defined as $C = \begin{bmatrix} \sqrt{\frac{k}{2}}I & 0 \end{bmatrix}$. Equivalently to the gyro bias observer, the UCO property is examined with output feedback, resulting in a persistency of excitation condition. If the following is true for any bounded $\omega_g(t)$, for any z in $\mathbb{R}^3$

$$z^T \Big[\int_t^{t+T_2} \Omega_g(\tau)^2 \Big] z > 0 \tag{43}$$

the system is UCO, and both $\tilde{\varepsilon}_o(t)$ and $\tilde{\gamma}_I(t)$ converge to zero exponentially fast. In other words, each component of $\omega_g(t)$ must be nonzero for some nontrivial interval over any interval of length T_2. (43) establishes the persistency of excitation (PE) condition for the scale factor observer.

Stability of Alignment Observer

Chose a Lyapunov function as

$$V_o(t) = \frac{1}{2} \begin{cases} (\tilde{\eta}_o(t) - 1)^2 + \tilde{\varepsilon}_o(t)^T \tilde{\varepsilon}_o(t) & \tilde{\eta}_o(t) \geq 0 \\ (\tilde{\eta}_o(t) + 1)^2 + \tilde{\varepsilon}_o(t)^T \tilde{\varepsilon}_o(t) & \tilde{\eta}_o(t) < 0 \end{cases}$$
$$+ \frac{1}{2} \begin{cases} (\tilde{\eta}_g(t) - 1)^2 + \tilde{\varepsilon}_g(t)^T \tilde{\varepsilon}_g(t) & \tilde{\eta}_g(t) \geq 0 \\ (\tilde{\eta}_g(t) + 1)^2 + \tilde{\varepsilon}_g(t)^T \tilde{\varepsilon}_g(t) & \tilde{\eta}_g(t) < 0 \end{cases} \tag{44}$$

After considerable manipulation, with the choices $k(t) = 4\|\omega_g(t)\| + k'$ and $k_1(t) = 6\|\omega_g(t)\| + k'_1$, with any $k' > 0$ and $k'_1 > 0$, the derivative of $V_o(t)$ can be written as

$$\dot{V}_o(t) \leq -k'\|\tilde{\varepsilon}_o(t)\|^2 - k'_1\|\tilde{\varepsilon}_o(t)\| \leq -k'\|\tilde{\varepsilon}_o(t)\|^2 \tag{45}$$

If $\omega_g(t)$ is bounded, $V_o(t)$ is a continuous, twice differentiable function. Barbalat's lemma then shows that $\|\tilde{\varepsilon}_o(t)\| \to 0$ as $t \to \infty$.[15]

The system given by (40) and (41) is stable. If $\omega_g(t)$ is bounded, all the signals are bounded. As with the gyro bias observer analysis, the system is cast as a linear time-varying system $\dot{x}(t) = A(t)x(t)$ where[14]

$$\mathbf{x(t)} = \begin{bmatrix} \tilde{\varepsilon}_o(t) \\ \tilde{\varepsilon}_g(t) \end{bmatrix}$$

In this case, developing $A(t)$ is more involved. Again, after considerable manipulation, the matrix $A(t)$ is written as

$$A(t) = \begin{bmatrix} A_{11}(t) & A_{12}(t) \\ A_{21}(t) & 0 \end{bmatrix}$$

where

$$A_{11}(t) = -\frac{1}{2} Q_1(\tilde{q}_o(t)) \text{sign}(\tilde{\eta}_o(t))[k + k_1 E]$$

$$A_{12}(t) = -Q_1(\tilde{q}_o(t))[(R(\hat{q}_g(t))\omega_g(t))\tilde{\varepsilon}_g(t)^T$$
$$- (\tilde{\varepsilon}_g(t)^T R(\hat{q}_g(t))\omega_g(t))I - \tilde{\eta}_g(t)S(R(\hat{q}_g(t))\omega_g(t))]$$

$$A_{21}(t) = -Q_1(\tilde{q}_g(t))[(R(\hat{q}_g(t))\omega_g(t))\tilde{\varepsilon}_o(t)^T$$
$$- (\tilde{\varepsilon}_o(t)^T R(\hat{q}_g(t))\omega_g(t))I - \tilde{\eta}_o(t)S(R(\hat{q}_g(t))\omega_g(t))]$$

where E is a diagonal matrix with the inverse of the absolute values of the components of $\tilde{\varepsilon}_o(t)$ on the main diagonal, $|\varepsilon(t)_i|^{-1}$. Again, as with the gyro bias and scale factor observers, the equilibrium point $x(t) = 0$ of this equivalent system is exponentially stable if the pair $(A(t), C)$ is uniformly

completely observable (UCO). Rewriting $\dot{V}_o(t)$ as $\dot{V}_o(t) \leq -x(t)^T C^T C x(t) \leq 0$, the matrix is C is defined as $C = [\sqrt{k'} \ 0]$. Examining the UCO properties, under output feedback, results in a persistency of excitation condition. Omitting the derivation details, if the following is true for a bounded $\omega_g(t)$, for any z in $\mathbb{R}^3$

$$z^T \Big[\int_t^{t+T_2} R(\tilde{q}_g(\tau))^T ((\omega(\tau)^T \omega(\tau)) I - \omega(\tau) \omega(\tau)^T) R(\tilde{q}_g(\tau)) d\tau \Big] z > 0 \qquad (46)$$

the system is UCO. In order to estimate the alignment errors, the angular velocity must change directions. Over any interval of length T_2, the angular velocity must not remain in a plane. If (46) is satisfied, the system is UCO, and the errors converge to zero exponentially fast. (46) establishes the persistency of excitation condition for the alignment observer.

CLOSED LOOP STABILITY

The nonlinear tracking control strategy proposed in Ref. 19 and summarized above cannot be implemented because exact measurements of the angular velocity $\omega(t)$ are not available. Instead, a certainty equivalence approach is proposed using estimates $\hat{\omega}(t)$ generated by the observer equations, resulting in

$$u(t) = -K_D \hat{s}(t) + H \hat{\alpha}_r(t) - S(H\hat{\omega}(t))\omega_r(t) \qquad (47)$$

where $\hat{s}(t) = \hat{\omega}(t) - \omega_r(t)$, $\hat{\bar{\omega}}_c(t) = \hat{\omega}(t) - R(\tilde{q}_c(t))\omega_d(t)$, and

$$\hat{\alpha}_r(t) = R(\tilde{q}_c(t))\dot{\omega}_d(t) - S(\hat{\bar{\omega}}_c(t))R(\tilde{q}_c(t))\omega_d(t) - \lambda Q_1(\tilde{q}_c(t))\hat{\bar{\omega}}_c(t)$$

Substitution of (47) into (19), the attitude dynamics, results in the following closed loop equation[20]

$$H\dot{s}(t) - S(H\omega(t))s(t) + K_D s(t) = \Delta(\tilde{q}_c(t), \omega_d(t))\tilde{s}(t) \qquad (48)$$

where $\Delta(\tilde{q}_c(t), \omega_d(t)) = -S(\omega_r(t))H - HS(R(\tilde{q}_c(t))\omega_d(t)) + \lambda HQ_1(\tilde{q}_c(t)) + K_D$. $\Delta(\tilde{q}_c(t), \omega_d(t))$ is a bounded matrix over any solution of the coupled dynamics (28) or (31), (29) or (30) or (32), (19), and (47).

In the case of gyro bias, the error term $\tilde{s}(t)$ is written as

$$\tilde{s}(t) = \omega(t) - \hat{\omega}(t) = -\tilde{b}(t)$$

The closed loop dynamics are then written as

$$H\dot{s}(t) - S(H\omega(t))s(t) + K_D s(t) = -\Delta(\tilde{q}_c(t), \omega_d(t))\tilde{b}(t) \qquad (49)$$

The control law (47) results in global stability and asymptotically perfect tracking, $\|\tilde{\varepsilon}_c(t)\| \rightarrow 0, \|\bar{\omega}_c(t)\| \rightarrow 0$. The proof is given in detail in Ref. 20.

Closed Loop Stability with Constant Scale Factor Error

Given the Lyapunov function $V_c(t) = s(t)^T H s(t)$, the derivative of $V_c(t)$, using (48), is

$$\dot{V}_c(t) = -s(t)^T K_D s(t) + s(t)^T \Delta(\tilde{q}_c(t), \omega_d(t))(s(t) - \hat{s}(t)) \qquad (50)$$

Rewriting the error term

$$\begin{aligned} s(t) - \hat{s}(t) = \omega(t) - \hat{\omega}(t) &= \Gamma^{-1}\omega_g(t) - \hat{\Gamma}_I(t)\omega_g(t) \\ &= \Gamma^{-1}\omega_g(t) - \hat{\Gamma}_I(t)\omega_g(t) \\ &= \tilde{\Gamma}_I(t)\omega_g(t) \end{aligned} \qquad (51)$$

9

Since

$$\omega_g(t) = \Gamma\omega(t) = \Gamma(s(t) + \omega_r(t)) \tag{52}$$

equation 51 is rewritten as

$$s(t) - \hat{s}(t) = \tilde{\Gamma}_I(t)\Gamma(s(t) + \omega_r(t)) \tag{53}$$

The convergence of $s(t)$ to zero depends on the exponential convergence of the scale factor errors, which in turn depends on the angular velocity $\omega_g(t)$ generated by the applied control. The derivative of $V_c(t)$ can be written, after some manipulation, as

$$\dot{V}_c(t) \le -\left(\frac{k_D}{2} - \zeta\|\gamma\|\|\tilde{\gamma}_I(t)\|\right)\|s(t)\|^2 + \frac{\zeta^2\|\gamma\|^2\omega_{r,max}^2}{2k_D}\|\tilde{\gamma}_I(t)\|^2 \tag{54}$$

where k_D is the smallest eigenvalue of K_D,

$$\zeta = \sup_{t \ge t_0} \sup_{\|\tilde{q}_c(t)\|=1} \|\Delta(\bar{q}_c(t), \omega_d(t))\| < \infty$$

and $\omega_{r,max}$ is the upper bound of $\|\omega_r(t)\| = \|R(\tilde{q}_c(t))\omega_d(t) - \lambda\bar{\varepsilon}_c(t)\| \le \|\omega_d(t)\| + \lambda$, since $\|\bar{\varepsilon}_c(t)\| \le 1$ and $\|R(\tilde{q}_c(t))\| = 1$. If k_D is sufficiently large, the closed loop system is uniformly, ultimately bounded. If the angular velocity, $\omega_g(t)$, in addition to being bounded (which ensures that the observer error terms are at least bounded), satisfies (43), the system is UCO and the scale factor errors converge to zero exponentially fast. In this case Theorem B.8 of Ref. 15 applies. $V_c(t)$ converges to zero exponentially fast, which means $s(t)$ converges to zero exponentially fast, regardless of the choice of k_D. With the convergence of $s(t) \to 0$, the proof of convergence of the actual attitude and rate errors follows exactly as in the gyro bias analysis of Ref. 20. The end result of which is $\lim_{t\to\infty}\|\bar{\varepsilon}_c(t)\| = 0$ and $\lim_{t\to\infty}\|\bar{\omega}_c(t)\| = 0$.

Closed Loop Stability with Constant Alignment Error

Again, using the Lyapunov function $V_c(t) = \frac{1}{2}s(t)^T H s(t)$, the derivative of $V_c(t)$ is

$$\dot{V}_c(t) = -s(t)^T K_D s(t) + s(t)^T \Delta(\bar{q}_c(t), \omega_d(t))\tilde{s}(t) \tag{55}$$

The error term $\tilde{s}(t)$ is rewritten as

$$s(t) - \hat{s}(t) = \omega(t) - \hat{\omega}(t) = \omega(t) - R(\hat{q}_g(t))\omega_g(t) = (I - R(\tilde{q}_g(t))^T)\omega(t)$$

Substituting $\omega(t) = s(t) + \omega_r(t)$ from equation 25, $\tilde{s}(t)$ is

$$\tilde{s}(t) = (I - R(\tilde{q}_g(t))^T)\omega(t) = (I - R(\tilde{q}_g(t))^T)(s(t) + \omega_r(t)) \tag{56}$$

The convergence of $s(t)$ to zero depends on the exponential convergence of the alignment errors, which in turn depends on the angular velocity $\omega(t)$ generated by the applied control. The derivative of $V_c(t)$ can be written, again, after some manipulation, as

$$\dot{V}_c(t) \le -\left(\frac{k_D}{2} - 2\zeta\|\bar{\varepsilon}_g(t)\|\right)\|s(t)\|^2 + \frac{2\zeta^2\omega_{r,max}^2}{k_D}\|\bar{\varepsilon}_g(t)\|^2 \tag{57}$$

where k_D, ζ, and $\omega_{r,max}$ are defined above. Again, if k_D is sufficiently large, the closed loop system is uniformly, ultimately bounded. If the angular velocity, $\omega(t)$, in addition to being bounded, satisfies (46), the system is UCO and the alignment errors, $\bar{\varepsilon}_g(t)$, converge to zero exponentially fast. As in the case of scale factor error, Theorem B.8 of Ref. 15 applies. $V_c(t)$ converges to zero exponentially fast, which means $s(t)$ converges to zero exponentially fast, regardless of the choice of k_D. With the convergence of $s(t) \to 0$, the proof of convergence of the actual attitude and rate errors follows exactly as in the gyro bias analysis of Ref. 20. The end result of which is $\lim_{t\to\infty}\|\bar{\varepsilon}_c(t)\| = 0$ and $\lim_{t\to\infty}\|\bar{\omega}_c(t)\| = 0$.

OBSERVER SIMULATION RESULTS

The observers are tested with a Matlab simulation. Table 1 lists the initial conditions for each observer, as well as the true states. The initial attitude quaternion and initial estimated attitude quaternion are the same for each observer test.

Observer State	Value	True State	Value
$\hat{q}(t_0)$	$[0,1,0,0]^T$	$q(t_0)$	$[0,0,1,0]^T$
$\hat{b}(t_0)$	$[0,0,0]^T \frac{deg}{sec}$	$b(t)$	$[2.9, -2.9, 1.9]^T \frac{deg}{sec}$
$\hat{\gamma}(t)$	$[1,1,1]$	γ	$[3, -5, 4]$
$\hat{q}_g(t)$	$[0,0,0,1]$	q_g	$[0,0,1,0]$

<p align="center">Table 1   Observer Simulation Initial Conditions</p>

First, results from the gyro bias observer are presented. The scale factors and alignment are known (and, without loss of generality, are each set to identity). The gain is chosen as $k = 1$. The angular velocity is $\omega(t) = [-5.7,\ 11.4,\ -22.9]$ deg/sec. Figure 1 shows $\|\bar{b}(t)\|$ converges to zero exponentially fast.
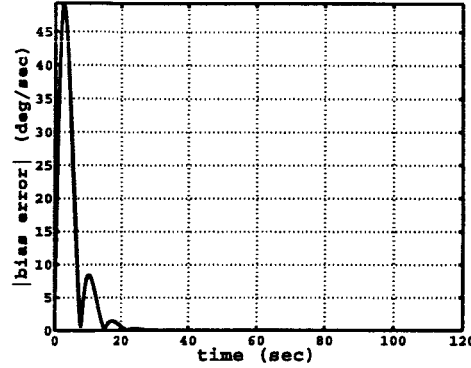

<p align="center">Figure 1   Observer Gyro Bias Error</p>

Next, results from the scale factor observer are presented. Here the gyro bias is zero, and the alignment matrix is the identity matrix. In the first case, the angular velocity is the same as in the gyro bias observer tests with $\omega(t)^T = [-5.7, 11.4, -22.9]$ deg/sec. Figure 2(a) shows that the scale factor errors, $\gamma_I - \hat{\gamma}_I(t)$, converge to zero. (Note that the inverse of the scale factor errors are plotted. Only the inverse of the estimate is used in the observer.)

In the second case, the x and y angular velocity components are as in the first case, but the z component is zero, $\omega(t) = [-5.7, 11.4, 0]$ deg/sec. Recall that the PE condition requires that all components of $\omega(t)$ be nonzero for UCO. Figure 2(b) shows that the scale factor errors for the x and y axes converge to zero, but the scale factor error for the z axis remains constant.

In the next case, the angular velocity components decrease exponentially $\omega(t) = [-5.7, 11.4, -22.9]e^{-t}$ deg/sec. This angular velocity does not meet the persistency of excitation condition of (43). Figure 2(c) shows that the scale factor errors do not converge to zero, but rather to constants.

<p align="center">11</p>

In the last case, angular velocity components switch between zero and $\omega_g(t) = [-5.7, 11.4, -22.9]$ deg/sec. A simple time interval is set up as

$$\omega_g(t) = \begin{cases} [-5.7, 11.4, -22.9] \text{ deg/sec} & t \in [n, n + 1/(n+1)] \\ [0, 0, 0] \text{ deg/sec} & t \in [n + 1/(n+1), n+1] \end{cases}$$

where

$$t_n = n, n = 1, 2, \ldots 200$$

This case also does not meet the UCO requirement of (43), since the angular velocity components are zero for progressively longer intervals. Figure 2(d) shows that the scale factor errors do not converge to zero, but rather are converging to constants.

(a) Constant Angular Velocity

(b) Zero Z Angular Velocity

(c) Exponential Angular Velocity

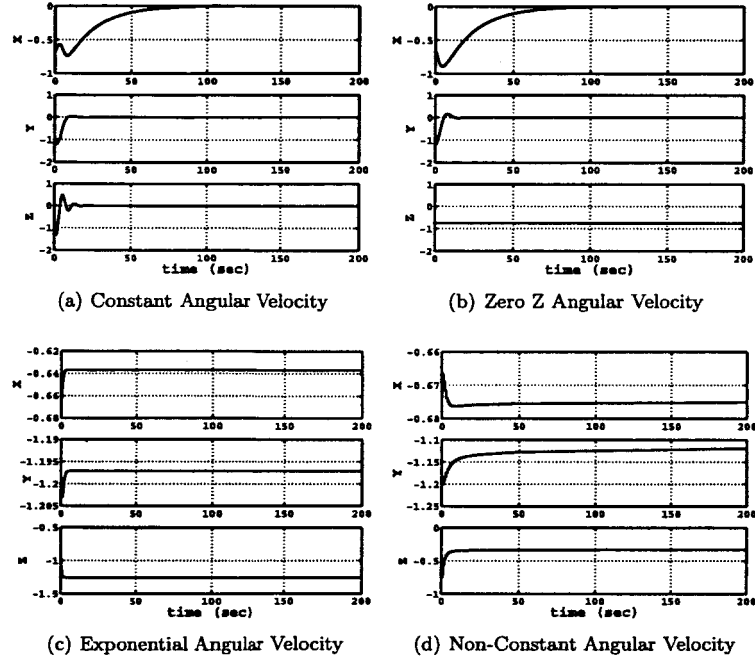(d) Non-Constant Angular Velocity

Figure 2 Scale Factor Observer Inverse Scale Factor Errors

Finally, results from the alignment observer are presented. The gyro bias is zero, and the scale factor matrix is the identity matrix. In the first case, the angular velocity is constant, with $\omega(t)^T = [0.1, 0.1, 0.1]$ deg/sec. The gains are chosen as $k' = 1$, $k'_1 = 0.001$. Figure 3(a) shows that the alignment errors converge to a constant, since a constant angular velocity does not meet the PE condition required by (46).

Next, the angular velocity is time varying. The angular velocity is

$$\omega(t)^T = [\cos \omega_m t, \sin \omega_m t, \cos 2\omega_m t] \text{deg/sec}$$

where $\omega_m = 2$ rad/sec. The gains are chosen as $k' = 0.001$ and $k'_1 = 0.1$. It can be shown that this angular velocity does meet the persistency of excitation condition of (46) for alignment errors. Figure 3(b) shows that alignment errors converge to zero.
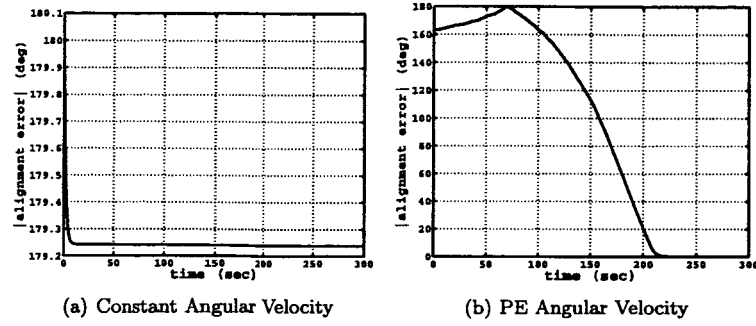
12

| (a) Constant Angular Velocity | (b) PE Angular Velocity |

Figure 3 Alignment Observer Alignment Error

Observer State	Value	True State	Value
$\hat{q}(t_0)$	$[0,0,0,1]^T$	$q(t_0)$	$[0,1,0,0]^T$
$\hat{b}(t_0)$	$[0,0,0]^T \frac{deg}{sec}$	$b(t)$	$[2.9,-2.9,1.9]^T \frac{deg}{sec}$
$\hat{\gamma}(t)$	$[1,1,1]$	γ	$[3,-5,4]$
$\hat{q}_g(t)$	$[0,0,0,1]^T$	q_g	$[0,0,0.3827,0.9238]^T$
		$q_d(t_0)$	$[0,0,0,1]^T$

Table 2 Closed Loop Simulation Initial Conditions

CLOSED LOOP SIMULATION RESULTS

The combined observers and controllers are also tested with a Matlab simulation. The inertia matrix is a diagonal matrix with principal moments of inertia chosen arbitrarily as $[90,100,70]\,\mathrm{kg\,m^2}$. The size of the principal moments of inertia is comparable to that of a small satellite. Table 2 lists the initial conditions for the observer and controller, as well as the true states. All the tests start with the same initial attitude quaternion, initial observer attitude quaternion, and initial desired attitude quaternion.

The combined observer/controller is first tested with a gyro bias. The gains are chosen as $k = 1$, $K_D = k_D I$, $k_D = 6$, and $\lambda = 3$. The desired trajectory is to track a 6.3 deg/sec rotation about the y-axis. The initial angular velocity is $\omega(t_0) = [-5.7, 11.4, -22.9]^T$ deg/sec. Figure 4(a) shows that $\|\tilde{b}(t)\|$ converges exponentially to zero. Figure 4(b) shows the tracking error, $\|\tilde{\varepsilon}_c(t)\|$, converges asymptotically to zero. Figure 4(c) similarly shows that the rate tracking errors converge to zero. Without correcting for the bias, the tracking error has a steady state error of approximately 30 degrees, as shown in Figure 4(d).

Next, the coupled observer/controller is tested with a scale factor error. The gains are chosen as $k = 1$, $K_D = k_D I_3$ (where I_3 indicates a 3x3 identity matrix), $k_D = 20$, and $\lambda = 0.1$. Here the initial angular velocity is $\omega(0)^T = [0,0,0]$, and the desired angular velocity is constant, $\omega_d(t)^T = [2.8, 2.8, 2.8]$ deg/sec. Figure 5(a) shows that the scale factor errors converge to zero. Figures 5(b) and 5(c) show that both the tracking attitude error and the tracking angular velocity error converge to zero. The controller is then run without correcting for the scale factor. Figure 5(d) shows the attitude tracking error, with the true scale factor reduced by a factor of 100 (the scale factor given in Table 2 produced tracking errors considerably larger). Without correcting for the scale factor,

13

(a) Bias Error

(b) Attitude Tracking Error

(c) Rate Tracking Error

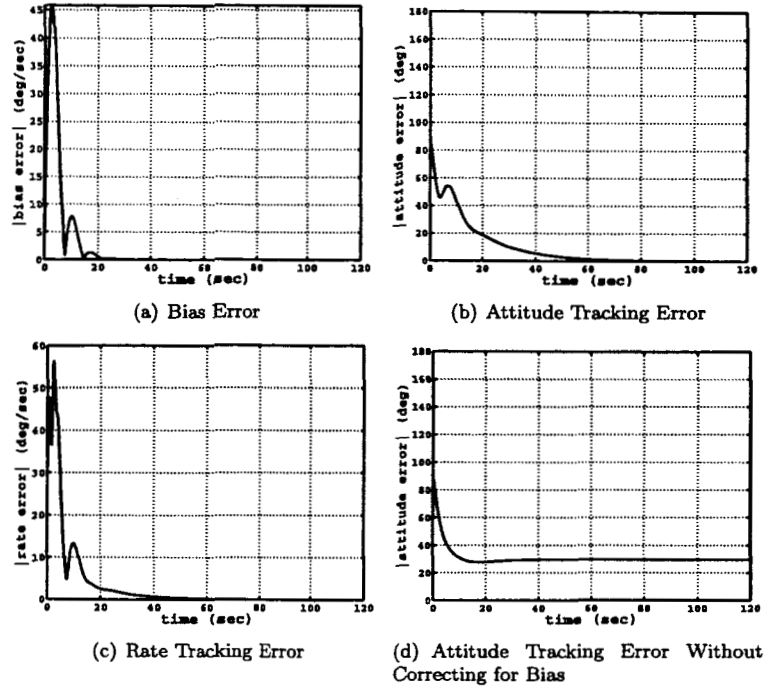(d) Attitude Tracking Error Without Correcting for Bias

Figure 4   Coupled Observer/Controller With Gyro Bias

the tracking errors do not converge.

Finally, the coupled observer/controller is tested with a constant alignment error. The gains are chosen as $k' = 0.1$, $k'_1 = 0.1$, $K_D = k_D I_3$ (where I_3 indicates a 3x3 identity matrix), $k_D = 20$, and $\lambda = 3$. The initial angular velocity is $\omega(0)^T = [0, 0, 0]$. The gyro coordinate frame is rotated by 45 degrees from the body frame, about the z-axis. The desired angular velocity changes direction, similarly to that used above to test just the observer, $\omega_d(t)^T = 5.73[\cos\omega_m t, \sin\omega_m t, \sin 2\omega_m t]$ deg/sec, with $\omega_m = 1$ deg/sec. Here, all the errors converge to zero. Figure 6(a) shows that the alignment errors converge to zero. Figures 6(b) and 6(c) show that that attitude and rate tracking errors converge to zero. Without correcting for the alignment, the attitude tracking error does not converge to zero, as shown in 6(d).

CONCLUSIONS

Three nonlinear observers for estimation of gyro bias, scale factor error, and alignment error are presented. All the observers are stable. The bias observer is exponentially stable. Both the scale factor and alignment observers are exponentially stable, but only under the condition that the angular velocity is bounded and meets a persistency of excitation condition. The persistency of excitation conditions are different for the scale factor observer and the alignment observer. For the scale factor observer, the angular velocity must be bounded and at least constant for regular time intervals. For the alignment observer, the angular velocity must be bounded, and must also change direction sufficiently in order to estimate the alignment.

Each observer is also coupled with a nonlinear control algorithm for attitude control of a rigid

14

(a) Scale Factor Inverse Error

(b) Tracking Attitude Error

(c) Tracking Rate Error

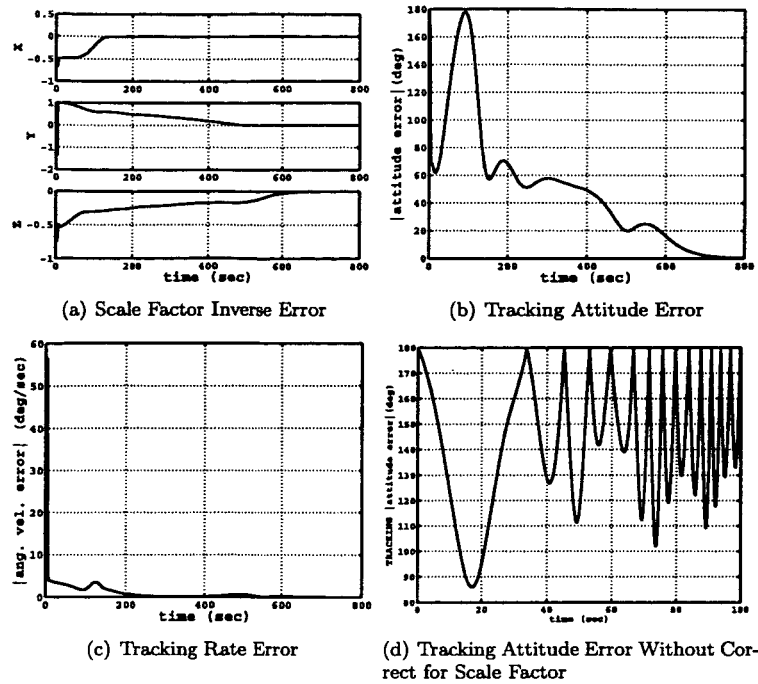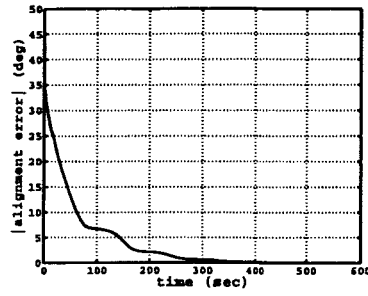(d) Tracking Attitude Error Without Correct for Scale Factor

Figure 5 Coupled Observer/Controller with Scale Factor Error

spacecraft. The coupled observer/controller in the case of bias error is stable. The tracking attitude and rate errors converge asymptotically to zero, and the bias errors converge exponentially to zero. The coupled observer/controller in the case of scale factor errors is stable, and converges asymptotically if the angular velocity is bounded and satisfies the pertinent persistency of excitation condition. The same is true for the coupled observer/controller in the case of an alignment error. The closed loop system is asymptotically stable if the angular velocity is bounded and meets the persistency of excitation condition for the alignment observer.

In this work, the three gyro observers are developed and tested independently. Since they are stable (exponentially stable under certain conditions) when examined alone, the next step is to understand the stability of simultaneously estimating combinations of bias, scale factor error and alignment error using the observers presented here. Future work will examine the stability of combining the observers, as a potential nonlinear gyro calibration utility. Additionally, the stability of combinations of the observers, coupled with a control algorithm, will be assessed. Uniformly bounded noise will also be considered in the analysis of the combined observers.

REFERENCES

1. Wertz, J. R., editor, *Spacecraft Attitude Determination and Control*, D. Reidel Publishing Company, 1984.

2. Deutschmann(now Thienel), J. K. and Bar-Itzhack, I., "Evaluation of Attitude and Orbit Estimation Using Actual Earth Magnetic Field Data," *AIAA Journal of Guidance, Control, and Dynamics*, Vol. 24, No. 3, May-June 2001, pp. 616–626.
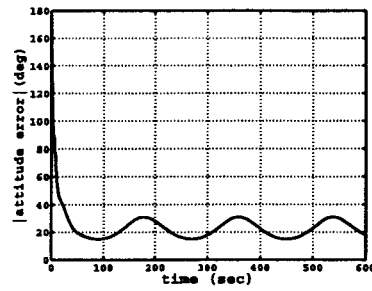
(a) Alignment Error
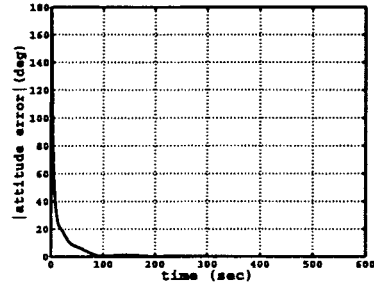
(b) Tracking Attitude Error
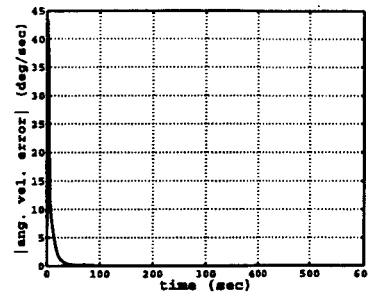
(c) Tracking Rate Error

(d) Tracking Attitude Error Without Correcting for Alignment

Figure 6 Coupled Observer/Controller with Alignment Error

3. Bar-Itzhack, I. and Harman, R. R., "In-Space Calibration of a Skewed Gyro Quadruplet," *AIAA Journal of Guidance, Control, and Dynamics*, Vol. 25, No. 5, September-October 2002, pp. 852–859.

4. Davenport, P. B. and Welter, G. L., "Algorithm for In-Flight Gyroscope Calibration," *Flight Mechanics/Estimation Theory Symposium*, NASA Goddard Space Flight Center, Greenbelt, Maryland, May 1988.

5. Welter, G., Boia, J., Gakenheimer, M., Kimmer, E., Channell, D., and Hallock, L., "Variations on the Davenport Gyroscope Calibration Algorithm," *Flight Mechanics/Estimation Theory Symposium*, NASA Goddard Space Flight Center, Greenbelt, Maryland, May 1996.

6. Hashmall, J. H., Radomski, M., and Sedlak, J., "On-Orbit Calibration of Satellite Gyroscopes," *AIAA/AAS Astrodynamics Specialist Conference*, Denver, Colorado, August 2000.

7. Filla, O. H., Willard, T. Z., Chu, D., and (now Thienel), J. D., "Inflight Estimation of Gyro Noise," *Flight Mechanics/Estimation Theory Symposium*, NASA Goddard Space Flight Center, Greenbelt, Maryland, May 1990.

8. Sedlak, J., Hashmall, J. H., and Airapetian, V., "Comparison of On-Orbit Performance of Rate Sensing Gyroscopes," *International Symposium on Spaceflight Dynamics*, Biarritz, France, June 2000.

9. Alonso, R., Crassidis, J. L., and Junkins, J. L., "Vision-Based Relative Navigation for Formation Flying of Spacecraft," *AIAA Guidance, Navigation, and Control Conference*, No. AIAA-2000-4439, Denver, Colorado, August 2000.

10. Salcudean, S., "A Globally Convergent Angular Velocity Observer for Rigid Body Motion," *IEEE Transactions on Automatic Control*, Vol. 36, No. 12, December 1991, pp. 1493–1496.

11. Vik, B., Shiriaev, A., and Fossen, T. I., "Nonlinear Observer Design for Integration of DGPS and INS," *New Directions in Nonlinear Observer Design*, Springer-Verlag, 1999.

12. Bošković, J. D., Li, S.-M., and Mehra, R. K., "A Globally Stable Scheme for Spacecraft Control in the Presence of Sensor Bias," *2000 IEEE Aerospace Conference*, Big Sky, Montana, March 2000.

13. Bošković, J. D., Li, S.-M., and Mehra, R. K., "Fault Tolerant Control of Spacecraft in the Presence of Sensor Bias," *American Control Conference*, Chicago, Illinois, March 2000.

14. Khalil, H. K., *Nonlinear Systems*, Prentice-Hall, Inc., 2nd ed., 1996.

15. Krstić, M., Kanellakopoulos, I., and Kokotovic, P., *Nonlinear and Adaptive Control Design*, John Wiley and Sons, Inc., 1995.

16. Shuster, M. D., "A Survey of Attitude Representations," *The Journal of Astronautical Sciences*, Vol. 41, No. 4, October-December 1993, pp. 439–517.

17. Sanner, R. M., "Adaptive Attitude Control Using Fixed and Dynamically Structured Neural Networks," *AIAA Guidance, Navigation, and Control Conference*, No. 96-3891, San Diego, California, July 1996.

18. Wie, B., *Space Vehicle Dynamics and Control*, AIAA Education Series, 1998.

19. Egeland, O. and Godhavn, J., "Passivity-Based Adaptive Attitude Control of a Rigid Spacecraft," *IEEE Transactions on Automatic Control*, Vol. 39, No. 4, April 1994, pp. 842–846.

20. Thienel, J. and Sanner, R. M., "A Coupled Nonlinear Spacecraft Attitude Controller and Observer with an Unknown Constant Gyro Bias and Gyro Noise," Accepted for publication in the IEEE Transactions on Automatic Control.